Available online at www.sciencedirect.com
SCIENCE DIRECT®
Advances in Space Research 34 (2004) 66–73
ADVANCES IN SPACE RESEARCH (a COSPAR publication)
www.elsevier.com/locate/asr

The heliospheric hydrogen wall and astrospheres

B.E. Wood [a,*], H.-R. Müller [b,c], G.P. Zank [c], V.V. Izmodenov [d], J.L. Linsky [a]

[a] University of Colorado and NIST, JILA, 440 UCB, Boulder, CO 80309-0440, USA
[b] Bartol Research Institute, University of Delaware, Newark, DE 19716, USA
[c] Institute of Geophysics and Planetary Physics, University of California at Riverside. 1432 Geology, Riverside, CA 92521, USA
[d] Department of Aeromechanics and Gas Dynamics. Faculty of Mechanics and Mathematics, Lomonosov Moscow State University, Moscow, 119899, Russia

Received 2 December 2002; received in revised form 28 December 2002; accepted 2 January 2003

Abstract

Charge exchange processes in the outer heliosphere produce a population of hot hydrogen gas within the heliosphere, creating a "hydrogen wall" between the heliopause and bow shock. The heliospheric hydrogen wall scatters Lyα photons passing through it, producing a detectable absorption signature in observations of H I Lyα emission from nearby stars. This heliospheric absorption has been observed using observations from the Hubble Space Telescope (HST), and these observations have also yielded detections of analogous "astrospheric" absorption from material surrounding the observed stars. The astrospheric detections dramatize the importance of understanding the heliospheric interaction, since similar interactions exist around other stars and can now be studied with HST. We review comparisons that have been made between the observed heliospheric absorption and the predictions of various models. The astrospheric absorption provides a way to empirically estimate the mass loss rates of solar-like stars, leading to the first empirical estimates of how solar-like winds vary with stellar age and activity. Thus, we also review these astrospheric results and discuss their ramifications for solar, stellar, and planetary science.

Keywords: Heliosphere; Heliospheric hydrogen wall; Charge exchange; H I Lyα emission

1. Introduction

Strong plasma interactions heat and compress interstellar protons just outside the heliopause. Thanks to charge exchange reactions between the protons and neutrals, these high temperatures and high densities are transmitted to the interstellar neutrals, creating what has been called a "hydrogen wall" of heated H I between the heliopause and bow shock (Baranov and Malama, 1993, 1995; Zank et al., 1996). The hydrogen wall is important because it is a structure in the outer heliosphere that can actually be detected and studied observationally, not only around the Sun but also around other stars (Linsky and Wood, 1996; Gayley et al., 1997; Wood et al., 1996; Wood et al., 2002a).

To be more precise, the heated heliospheric H I creates a detectable absorption signature in the H I Lyman-α lines observed by the Hubble Space Telescope (HST) from nearby stars. The models show that hot heliospheric H I actually permeates the entire heliosphere, but because of the high densities in the hydrogen wall, it is the hydrogen wall that dominates the Lyα absorption for most lines of sight. In this paper, we review what the Lyα absorption data have taught us about the heliosphere and astrospheres, where we use the term "astrosphere" as the stellar analog of the heliosphere. The astrospheric work will be particularly emphasized here, because astrospheric detections allow us to study the winds of solar-like stars, which have never been observable before. This broadens the importance of understanding the heliosphere and its physical processes, because similar wind–ISM interaction regions also exist around other solar-like stars and currently these interaction regions provide the only way to study the winds of these stars.

* Corresponding author. Tel.: +1-303-492-7820; fax: +1-303-492-5235.
E-mail address: woodb@origins.colorado.edu (B.E. Wood).

0273-1177/$30 © 2004 COSPAR. Published by Elsevier Ltd. All rights reserved.
doi:10.1016/j.asr.2003.01.035

2. The heliospheric absorption

Fig. 1 shows the H I Lyα line observed by HST from α Cen B, a K0 V star located at a distance of only 1.3 pc. This star is a member of the closest star system to the Sun, which includes also α Cen A (G2 V) and a very distant companion, Proxima Cen (M5.5 V). Even towards this nearest star system, there exists enough interstellar neutral hydrogen (H I) along the line of sight to produce a very broad absorption line that obliterates the center of the stellar Lyα emission line (see Fig. 1). There is also enough deuterium (D I) to produce a narrow D I absorption feature −0.33 Å from the center of the H I absorption.

Observations of Lyα have been made for many nearby stars, first using the Goddard High Resolution Spectrograph (GHRS) instrument on HST, and then using the Space Telescope Imaging Spectrograph (STIS), which replaced the GHRS in 1997. The primary purpose of these observations was to study the properties of the local interstellar medium (LISM) using interstellar absorption lines like the H I and D I lines shown in Fig. 1. One quantity of particular interest is the D/H ratio in the LISM, because of the importance of this quantity for cosmology and for testing our understanding of Galactic chemical evolution.

Initial attempts to model the α Cen Lyα absorption in Fig. 1 were frustrated by inconsistency between the H I absorption and the other ISM absorption lines. The H I absorption is redshifted relative to the other lines by 2.2 km s^{-1}, and its width is too broad to be consistent with the $T = 5400 \pm 500$ K temperature suggested by the width of the D I line (Linsky and Wood, 1996). Attempts to mitigate this problem by fiddling with the assumed stellar Lyα profile (see Fig. 1) were completely unsuccessful. The only way the H I absorption feature could be fitted in a self-consistent manner with D I was to propose that there is excess absorption on both sides of the H I Lyα absorption feature that is from a different origin than the LISM absorption seen in D I and other lines.

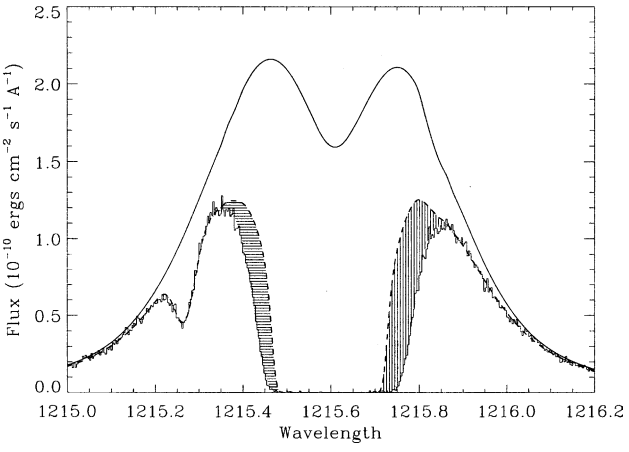

Fig. 1. HST/GHRS Lyα spectrum of α Cen B, showing broad H I absorption at 1215.6 Å and D I absorption at 1215.25 Å. The upper solid line is the assumed stellar emission profile and the dashed line is the ISM absorption alone. The excess absorption is due to heliospheric H I (vertical lines) and astrospheric H I (horizontal lines). From Linsky and Wood (1996).

Fortuitously, the first models of the heliosphere treating the interstellar neutrals and plasma in a self-consistant manner were being developed and published at about that time (Baranov and Malama, 1993, 1995; Zank et al., 1996), and these models provided a fascinating explanation for this excess H I absorption. Perhaps the absorption was from heated heliospheric H I, most of it in the hydrogen wall. Even though heliospheric H I column densities are three orders of magnitude lower than LISM column densities towards even the nearest stars, the high temperature of the heliospheric H I allows it to produce an absorption line broad enough to extend beyond the LISM absorption. Thus, Linsky and Wood (1996) proposed that heliospheric absorption was primarily responsible for the excess absorption, but they speculated that astrospheric absorption from material around α Cen could in principle also be contributing.

Gayley et al. (1997) were the first to make a direct comparison between the α Cen Lyα data and heliospheric model predictions. Their work made it clear that the heliospheric models could indeed reproduce the excess absorption on the red-side of the Lyα line, but *not* the blue-side excess (see Fig. 1). They showed that absorption from astrospheric material was required to account for the blue-side excess. Further work has shown that heliospheric absorption generally produces excess absorption only on the red-side of the line regardless of the line of sight (Izmodenov et al., 1999; Wood et al., 2000b), while astrospheric absorption only results in substantial blue-side absorption. The primary reason for this convenient separation is the deceleration and deflection of LISM material as it crosses solar/stellar bow shocks. For the heliosphere, where we are observing from inside the wind/LISM interaction, the result is redshifted absorption relative to the LISM absorption, while for astrospheres, where we are observing from outside the interaction, the result is blueshifted absorption.

The line of sight to α Cen is $\theta = 52°$ from the upwind direction of the LISM flow seen by the Sun, meaning that the heliospheric absorption seen in the HST data is from a generally upwind part of the heliosphere. By now, excess red-side absorption that is believed to be heliospheric in origin has been detected for other lines of sight: 36 Oph ($\theta = 12°$; Wood et al., 2000a), Sirius ($\theta = 139°$; Izmodenov et al., 1999), and possibly HZ 43 ($\theta = 70°$; Kruk et al., 2002). There are more subtle suggestions of some heliospheric contribution to the H I

absorption observed towards Capella and G191-B2B (Vidal-Madjar et al., 1998; Lemoine et al., 2002). The Sirius detection is notable for being a downwind line of sight in which much of the absorption will be from heated H I in the heliotail rather than the hydrogen wall.

Recent work on the heliospheric Lyα absorption has focused on determining the extent to which the absorption can be used as a diagnostic for various properties of the LISM, and on determining whether heliospheric models of various types can simultaneously fit absorption observed for different directions by HST (see Fig. 2). Wood et al. (2000b) compared Lyα absorption predictions of various kinetic, or "Boltzmann," models of the type described by Müller et al. (2000) with the HST data, not only for three lines of sight with detected heliospheric absorption (α Cen, 36 Oph, and Sirius), but for three other observed lines of sight (31 Com, β Cas, and ε Eri). No heliospheric absorption is detected towards these last three stars, but the data provide useful upper limits for the amount of absorption that can be present in those directions. The primary LISM parameter that was varied was a parameter relating the proton pressure to the total LISM pressure: high values correspond to a LISM with substantial magnetic field and/or cosmic ray pressure. It was found that the Boltzmann models tend to predict too much absorption, especially in downwind directions, and no Boltzmann model was found that could simultaneously fit all the data.

Although the Boltzmann models are not entirely successful in fitting the Lyα data, Wood et al. (2000b) found that a four-fluid code, of the type described by Zank et al. (1996), could fit the data, including the downwind directions. The four-fluid code assumes that the H I velocity distributions can be represented by the sum of three Maxwellian H-fluids, one for each distinct region where charge exchange takes place (between the heliopause and bow shock, between the termination shock and heliopause, and inside the termination shock), plus one-fluid for the H^+. The apparent greater success of the four-fluid code compared to the kinetic code is surprising since unlike the four-fluid code the kinetic models make no a priori assumptions at all about the shape of the velocity distributions. Nevertheless, Fig. 2 shows the predictions of a four-fluid code, which fit the data reasonably well. The input LISM

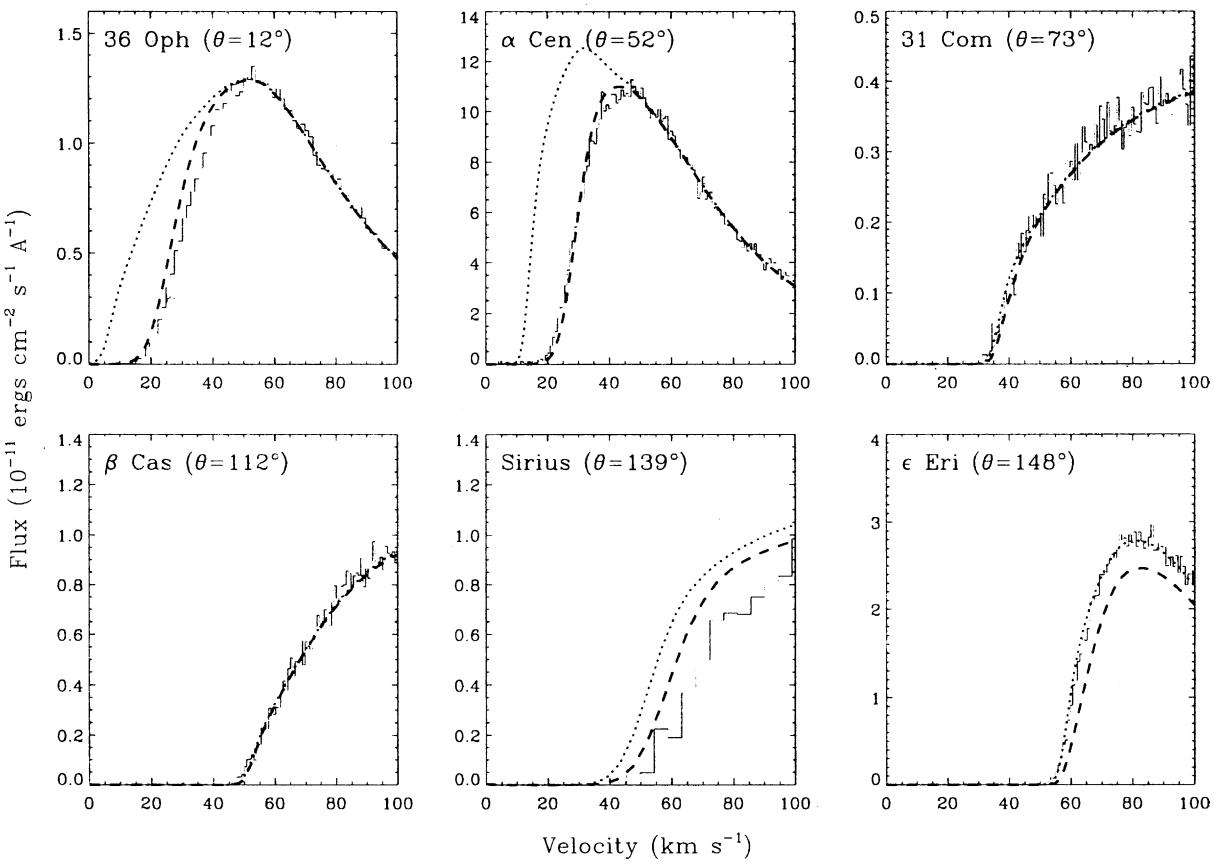

Fig. 2. Comparison of the H I absorption predicted by a four-fluid heliospheric model and HST observations of six lines of sight, where we have zoomed in on the red-side of the H I Lyα lines. The dotted lines show the ISM absorption alone and the dashed lines show the total Lyα absorption after the model heliospheric absorption is added to the ISM absorption. Reasonably good agreement is observed, although there is a slight underprediction of absorption towards 36 Oph and Sirius, and a slight overprediction towards ε Eri. From Wood et al. (2000b).

parameters for this model are: $V = 26$ km s^{-1}, $n(H^+) = 0.1$ cm^{-3}, $n(H\ I) = 0.14$ cm^{-3}, and $T = 8000$ K. The assumed solar wind parameters at 1 AU are: $V = 400$ km s^{-1}, $n(H^+) = 5$ cm^{-3}, and $T = 10^5$ K (Wood et al., 2000b).

Izmodenov et al. (2002) have also used *their* kinetic models, of the type described by Baranov and Malama (1993, 1995) to compare model predictions with these same data. They find they can nicely fit upwind and sidewind directions with reasonable input LISM parameters, but like Wood et al. (2000b) they also find difficulties with fitting downwind directions. One possible reason for the difficulties the kinetic models seem to have with downwind directions is an overly simplistic single-fluid treatment of protons within the termination shock, in which pickup ions are grouped with undisturbed solar wind protons into a single plasma component. Izmodenov et al. (2002) propose that this approximation may lead to inaccurate velocity distribution functions in the heliotail region especially, resulting in the overpredictions of H I absorption. In the future, a multi-fluid approach to modeling the plasma could test this idea.

For upwind and sidewind directions (i.e., for $\theta < 120°$), Izmodenov et al. (2002) find surprisingly little variability in predicted Lyα absorption when the interstellar hydrogen and proton densities are varied. If the LISM hydrogen density is increased, for example, the H I density within the hydrogen wall increases, but the higher LISM ram pressure makes the hydrogen wall narrower. Thus, the H I column density through the hydrogen wall does not change greatly and neither does the amount of Lyα absorption. The ionization fraction also does not have as much effect as one might suppose. This means that the Lyα absorption may not be as sensitive a diagnostic of LISM densities as we would like, but this is actually good news for the astrospheric work described in the next section. In modeling astrospheres, one must assume that LISM parameters do not vary greatly from star to star. The results of Izmodenov et al. (2002) suggest that even if there *are* modest variations of LISM parameters, the absorption predictions of astrospheric models will not be greatly compromised.

3. The astrospheric absorption

Even before Gayley et al. (1997) showed that a contribution from astrospheric absorption was required to account for all the excess H I Lyα absorption detected towards α Cen, additional detections of excess Lyα absorption were found that were immediately interpreted as being predominantly astrospheric rather than heliospheric in nature (Wood et al., 1996; Dring et al., 1997). These excesses were solely on the blue-side of the Lyα line, and it was already understood that heliospheric hydrogen will produce absorption that is at least mostly redshifted. Since the α Cen situation was not resolved until the work of Gayley et al. (1997), the first detections of atmosperic absorption should probably be considered to be that of ε Ind and λ And (Wood et al., 1996), although the λ And detection should be regarded as somewhat questionable (Wood et al., 2002a). Several other astrospheric detections followed shortly thereafter (Dring et al., 1997; Wood and Linsky, 1998; Wood et al., 2000a).

The strongest purely empirical evidence that astrospheric material is responsible for the blue-side excess Lyα absorption comes from comparing the Lyα profiles of α Cen and a distant companion star called Proxima Cen. The blue-side excess seen toward α Cen is not seen towards Proxima Cen. Since the two lines of sight are practically identical, the blue-side excess absorption towards α Cen cannot be from some mysterious LISM or heliospheric absorption component. It must instead be from circumstellar material surrounding α Cen that does not extend as far as the distant ($\sim$12,000 AU away) companion Proxima Cen, consistent with the astrospheric interpretation (Wood et al., 2001).

The astrospheric detections collectively represent the first detections, albeit indirect, of winds around solar-like stars, and have led to the first mass loss measurements of these stars. Therein lies their importance, for the astrospheric absorption provides us with our first opportunity to study how the properties of solar-like winds vary with stellar age and activity. This is possible because the amount of absorption depends on the stellar mass loss rate, since larger mass loss rates will lead to larger astrospheres and larger astrospheric H I column densities, and therefore more absorption.

Table 1 lists mass loss rates that have been estimated for all stars with detected astrospheric absorption (Wood et al., 2001, 2002a; Müller et al., 2001). In some binary star systems, such as α Cen and 36 Oph, both members of the binary are within the same astrosphere and therefore the mass loss measurement is indicative of the combined mass loss of both stars. In those cases, the spectral types of both stars are listed, and the stellar surface area listed (last column) is the combined surface area of both stars. The V_{ISM} and θ parameters listed in the table are the LISM wind speed seen by the star and the angle of our line of sight to the star with respect to the upwind direction of the ISM flow seen by the star, taking into account the unique proper motions of each star through the local ISM. The mass loss estimates are listed in solar units, and the second-to-last column lists logarithmic stellar X-ray luminosities (in erg s^{-1}).

Making the stellar mass loss measurements requires the use of astrospheric models. Fig. 3 compares the α Cen data with the astrospheric absorption predicted by four models of the α Cen astrosphere assuming different mass loss rates (Wood et al., 2001). The

Table 1
Astrospheric mass loss measurements

Star	Spectral type	d (pc)	V_{ISM} (km s^{-1})	θ (°)	$\dot{M}$ ($\dot{M}_\odot$)	Log L_x	Surface area ($A_\odot$)
α Cen	G2 V + K0 V	1.3	25	79	2	27.34	2.37
Proxima Cen	M5.5 V	1.3	25	79	<0.2	27.23	0.026
ε Eri	K1 V	3.2	27	76	30	28.32	0.62
61 Cyg A	K5 V	3.5	86	46	0.5	27.26	0.45
ε Ind	K5 V	3.6	68	64	0.5	27.18	0.50
36 Oph	K1 V + K1 V	5.5	40	134	15	28.28	0.88
λ And[a]	G8 IV-III + M V	26	53	89	5	30.48	55

[a] Questionable astrospheric detection.

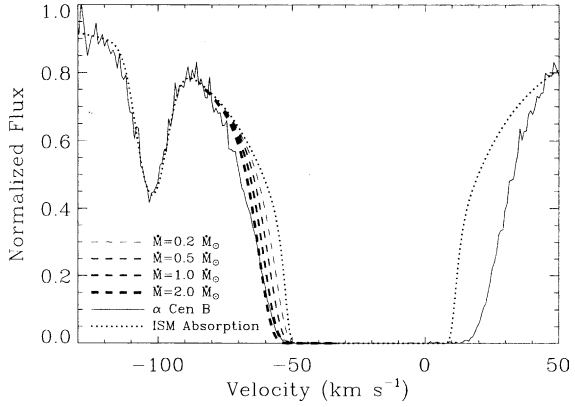

Fig. 3. The α Cen B spectrum (thin solid line) and inferred ISM absorption (dotted line) from Fig. 1. The dashed lines show the blue-side excess Lyα absorption predicted by four models of the α Cen astrosphere, assuming four different mass loss rates. The 2.0 $\dot{M}_\odot$ model fits the α Cen spectrum reasonably well. From Wood et al. (2001).

$\dot{M} = 2\ \dot{M}_\odot$ model fits the data best, so that is the mass loss rate estimate for α Cen reported in Table 1. Since the model used to predict the heliospheric absorption in Fig. 2 is at this point the best predictor of heliospheric absorption, that four-fluid model has been used as the starting point for all the astrospheric models. For example, in order to change that $\dot{M} = 1\ \dot{M}_\odot$ heliospheric model to a $\dot{M} = 2\ \dot{M}_\odot$ α Cen model, we merely recompute the heliospheric model with the ISM wind speed changed to the appropriate V_{ISM} value for α Cen listed in Table 1 and increase the assumed wind proton density by a factor of 2. All the other input parameters (which were listed in the previous section) remain the same. In the future, we hope to try to use kinetic models to measure mass loss rates, for comparison with the ones in Table 1 derived using four-fluid models.

Note that the astrospheric detection of λ And is flagged as uncertain in Table 1, because there are no observations of narrow ISM lines such as Mg II h and k to provide information on the velocity structure of the ISM for that line of sight. As a consequence, the Lyα lines are analyzed assuming a single absorption component. This analysis clearly suggests the presence of excess H I absorption on the blue-side of the line, but without knowledge of the ISM velocity structure it remains possible that there is a blueshifted ISM component that might be able to account for the H I excess without requiring an astrospheric component.

There was another astrospheric detection, 40 Eri A, which had been considered uncertain and had a derived mass loss upper limit of $\dot{M} < 5\ \dot{M}_\odot$ (Wood et al., 2002a). However, there was an attempt to detect astrospheric Lyα *emission* surrounding this star that proved unsuccessful, and it has since been argued that the questionable detection of astrospheric absorption towards 40 Eri A is inconsistent with this nondetection (Wood et al., 2002b). Thus, 40 Eri A has now been removed entirely from the list of stars with detected astrospheric absorption (see Table 1).

The winds of solar-like stars have their origins in the coronae of these stars, so it is natural to consider whether mass loss rates are correlated with coronal properties. The coronal X-ray luminosity is a good indicator of the magnetic activity level of a star and of the amount of material that has been heated to high coronal temperatures. Table 1 lists X-ray luminosities obtained with the *ROSAT* PSPC instrument, and in Fig. 4 the mass loss per unit surface area (in solar units) is plotted versus X-ray surface flux (F_X). The Sun is included assuming an average X-ray luminosity of $\log L_x = 27.3$, although this value can be about a factor of 2 higher or lower due to solar cycle variability (Ayres, 1997). Presumably the other stars vary in a similar fashion. For the solar-like GK dwarfs, the data suggest that the more active stars have higher mass loss rates (Wood et al., 2002a). It is uncertain why the M dwarf Proxima Cen and the RS CVn system λ And (G8 IV-III + M V) have mass loss rates that are much lower than one would expect based on the mass loss/activity relation defined by the solar-like stars. Is this due to the different surface gravities of these stars, the generally higher coronal temperatures, stronger magnetic fields, or something else?

If we ignore Proxima Cen and λ And, and focus only on the more solar-like GK dwarfs, we can fit a power law to the data in Fig. 4, which suggests that

$$\dot{M} \propto F_x^{1.15\pm0.20}, \tag{1}$$

where the error bar is estimated assuming factor of 2 uncertainties in the mass loss rates and factor of 2

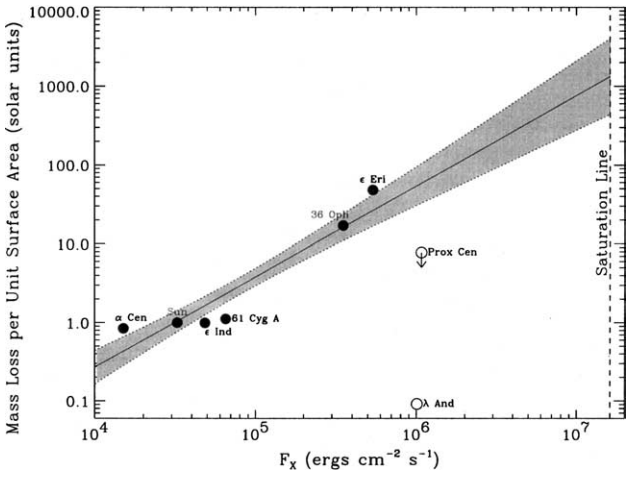

Fig. 4. Measured mass loss rates (per unit surface area) plotted versus X-ray surface flux. A power law has been fitted to the solar-like GK dwarfs (filled circles), and the shaded region is the estimated uncertainty in the fit. Proxima Cen (M5.5 Ve) and λ And (G8 IV-III + M V) appear to be inconsistent with this relation. The saturation line represents the maximum F_X value observed for solar-like stars. From Wood et al. (2002a).

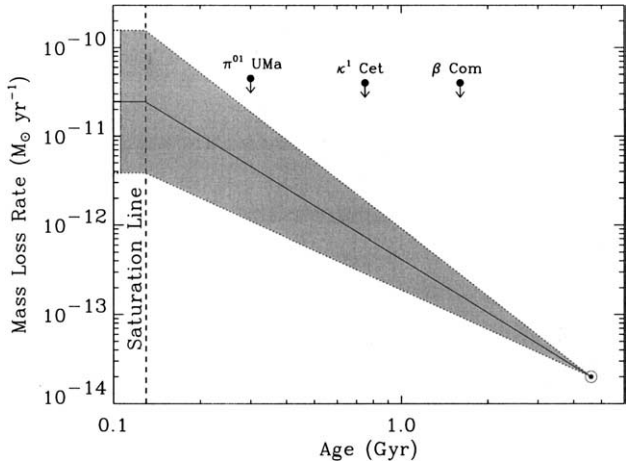

Fig. 5. The mass loss history of the Sun as suggested by the power law relation from Fig. 4 and the age versus activity relation from Ayres (1997). The upper limits are based on radio nondetections of three solar-like stars (Gaidos et al., 2000). From Wood et al. (2002a).

uncertainties in the X-ray fluxes (due to variability). In the figure, this relation is extrapolated up to a saturation line, which represents the maximum X-ray flux observed for solar-like stars (Güdel et al., 1997).

The assumption is that when the coronal X-ray flux saturates, the wind will also. Fig. 4 suggests that a coronally saturated star should have a mass loss rate about 1000 times larger than that of the Sun. It is known from previous observational work that coronal activity increases with the stellar rotation velocity ($V_{\rm rot}$), which declines with time (t) due to magnetic braking. Combining power law relations between F_X, $V_{\rm rot}$, and t from Ayres (1997) with our mass loss/activity relation in Eq. (1), we can derive

$$\dot{M} \propto t^{-2.00\pm0.52}. \tag{2}$$

This is the first observationally derived relation between mass loss and age for solar-like stars. Fig. 5 shows what this relation suggests for the mass loss history of the Sun. The solar wind may have been ~1000 times stronger when the Sun was very young, although predictions for very early times are suspect (Wood et al., 2002a). The upper limits in Fig. 5 are based on nondetections of radio emission from three solar-like stars (Gaidos et al., 2000), illustrating that the high mass loss rates predicted for young stars are still consistent with our inability to detect radio emission from these stars.

4. Implications of the derived wind evolution relation

The stellar wind evolution relation derived in Eq. (2) has important ramifications for both solar/stellar physics and planetary science (Wood et al., 2002a). We now discuss a few of these implications.

4.1. Magnetic braking

Stellar rotation rates decrease with time due to a braking effect whereby the magnetic field of the star drags against the stellar wind as the star rotates. The amount of drag naturally depends on the density of the wind and therefore the mass loss rate. Theoretically, the magnetic braking law has been expressed as

$$\frac{\dot{\Omega}}{\Omega} \propto \frac{\dot{M}}{M}\left(\frac{R_A}{R}\right)^m, \tag{3}$$

where Ω is the angular rotation rate (Stepień, 1988; Gaidos et al., 2000). The Alfvén radius, R_A, is

$$R_A = \sqrt{\frac{V_w \dot{M}}{B_r^2}}, \tag{4}$$

where V_w is the stellar wind speed and B_r is the disk-averaged, radial component of the magnetic field. The exponent m in Eq. (3) is a number between 0 and 2, where $m = 2$ corresponds to a purely radial magnetic field. Mestel (1984) argues that more reasonable magnetic geometries suggest $m = 0$–1.

If one assumes that R, M, and V_w are time invariant, we can plug Eq. (2) into Eq. (3) to derive an expression describing how stellar magnetic fields must evolve with time according to the theoretical magnetic braking law. If $B_r \propto t^\alpha$, we find that

$$\alpha = 1/m - (1.00 \pm 0.26)(m+2)/m. \tag{5}$$

The physically allowable range of $m = 0$–2 suggests $\alpha < -1.0$, while the more likely range of $m = 0$–1 suggested by Mestel (1984) implies $\alpha < -1.2$. In any case,

the bottom line is that the theoretical description of magnetic braking described above is consistent with our mass loss evolution law only if disk-averaged stellar magnetic fields decrease at least inversely with age for solar-like stars.

4.2. The faint young Sun paradox

Another application of our mass loss evolution law concerns the "faint young Sun paradox." Our understanding of stellar evolution and stellar interiors suggests that the Sun should have been about 25% fainter than today about 3.9 Gyr ago (e.g., Bahcall et al., 2001), but as first realized by Sagan and Mullen (1972) this is a problem for planetary geologists. If the Sun were 25% fainter, the planets should have been correspondingly cooler. Earth and Mars should have been too cold for liquid water to exist on their surfaces, but this contradicts evidence that liquid water *did* in fact exist on both planets.

Most attempts to explain the faint young Sun paradox have assumed that the solution lies in greater greenhouse gases in the planetary atmospheres in the early solar system that compensated for the fainter Sun. However, this interpretation has some difficulties and an alternative explanation that has been proposed is that perhaps the young Sun was more massive than today, allowing it to be more luminous than one would normally expect it to be (Gough, 1981). Recent calculations by Sackmann and Boothroyd (2003) suggest that the Sun must have been at least about 2% more massive 3.9 Gyr ago to solve the faint young Sun paradox. In order for this proposal to work, the mass loss rate of the young Sun must have been much higher than today to reduce the Sun's mass to its present value. This is where our mass loss evolution law enters the picture. The power law relation in Eq. (2) does suggest that the Sun had a significantly higher mass loss rate in the distant past. Unfortunately, the mass loss is highly peaked towards very early times. By 3.9 Gyr ago, the predicted mass loss rate had already fallen too low for there to be much mass loss after that. To be more precise, Eq. (2) suggests that 3.9 Gyr ago the Sun could have been no more than about 0.1% more massive than today, an order of magnitude lower than the 2% required by Sackmann and Boothroyd (2003). Thus, a more massive young Sun is not a likely solution to the faint young Sun paradox.

4.3. Solar wind erosion

Even if a more massive young solar wind is not the solution to the faint young Sun problem, the eroding effects of such a wind may still have had profound effects on planetary atmospheres in our solar system. The effects of solar wind sputtering processes have been explored for both Venus and Titan (Chassefière, 1997; Lammer et al., 2000). However, the Martian atmosphere may be the most dramatic case of solar wind erosion, because solar wind erosion on Mars may have led to the loss of most of its atmosphere, resulting in the disappearance of water, and perhaps even life, from the surface of the planet.

Like Earth, Mars apparently once had a global magnetic field that protected its atmosphere from the solar wind, but that magnetic field disappeared at least 3.9 Gyr ago (Acuña et al., 1999). The Martian atmosphere would have then been exposed to a solar wind about 40 times stronger than the current wind according to Fig. 5. The current Martian atmosphere is much too thin for surface water to be stable, but Mars appears to have had running water on its surface in the distant past, and there is evidence from isotopic ratios in the Martian atmosphere that Mars once had a thicker atmosphere that could have allowed a climate much more conducive to the existence of surface water (e.g., Carr, 1996). Solar wind erosion is a leading candidate for the cause of this dramatic change (e.g., Kass and Yung, 1995). The higher mass loss rates predicted for the young solar wind in Fig. 5 make it even more likely that the solar wind has played a crucial role in the evolution of planetary atmospheres such as that of Mars.

Acknowledgements

Support was provided by NASA through Grants NAG5-9041 and S-56500-D to the University of Colorado. G.P.Z. and H.-R.M. would also like to acknowledge support from NSF-DOE Grant ATM-0296114.

References

Acuña, M.J., Connerney, J.E.P., Ness, N.F., et al. Global distribution of crustal magnetism discovered by the Mars Global Surveyor MAG/ER experiment. Science 284, 790–793, 1999.

Ayres, T.R., Evolution of the solar ionizing flux, J. Geophys. Res. 102, 1641–1652, 1997.

Bahcall, J.N., Pinsonneault, M.H., Basu, S. Solar models: current epoch and time dependences, neutrinos, and helioseismological properties. Astrophys J. 555, 990–1012, 2001.

Baranov, V.B., Malama, Y.G. Model of the solar wind interaction with the local interstellar medium – numerical solution of self-consistent problem. J. Geophys. Res. 98, 15157–15163, 1993.

Baranov, V.B., Malama, Y.G. Effect of local interstellar medium hydrogen fractional ionization on the distant solar wind and interface region. J. Geophys. Res. 100, 14755–14762, 1995.

Carr, M.H. Water on Mars. Oxford University Press, New York, USA, 1996.

Chassefière, E. Loss of water on the young Venus: the effect of a strong primitive solar wind. Icarus 126, 229–232, 1997.

Dring, A.R., Linsky, J., Murthy, J., et al. Lyman-α absorption and the D/H ratio in the local interstellar medium. Astrophys. J. 488, 760–775, 1997.

Gaidos, E.J., Güdel, M., Blake, G.A. The faint young Sun paradox: an observational test of an alternative solar model. Geophys. Res. Lett. 27, 501–503, 2000.

Gayley, K.G., Zank, G.P., Pauls, H.L., et al. One-versus two-shock heliosphere: constraining models with GHRS Lyman-α spectra toward α Centauri. Astrophys. J. 487, 259–270, 1997.

Gough, D.O. Solar interior structure and luminosity variations. Solar Phys. 74, 21–34, 1981.

Güdel, M., Guinan, E.F., Skinner, S.L. The X-ray Sun in time: a study of the long-term evolution of coronae of solar-type stars. Astrophys. J. 483, 947–960, 1997.

Izmodenov, V.V., Lallement, R., Malama, Y.G. Heliospheric and astrospheric hydrogen absorption towards Sirius: no need for interstellar hot gas. Astron. Astrophys. 342, L13–L16, 1999.

Izmodenov, V.V., Wood, B.E., Lallement, R. Hydrogen wall and heliosheath Lyman-α absorption toward nearby stars: possible constraints on the heliospheric interface plasma flow. J. Geophys. Res. 107, 1308–1322, 2002.

Kass, D.M., Yung, Y.L. Loss of atmosphere from Mars due to solar wind-induced sputtering. Science 268, 697–699, 1995.

Kruk, J.W., Howk, J.C., André, M., et al. Abundances of deuterium, nitrogen, and oxygen toward HZ 43A: results from the FUSE mission. Astrophys. J. Supp. 140, 19–36, 2002.

Lammer, H., Stumptner, W., Molina-Cuberos, G.J., et al. Nitrogen isotope fractionation and its consequence Titan's atmospheric evolution. Planet. Space Sci. 48, 529–543, 2000.

Lemoine, M., Vidal-Madjar, A., Hébrard, G., et al. Deuterium abundance toward G191-B2B: results from the FUSE mission. Astrophys. J. Supp. 140, 67–80, 2002.

Linsky, J.L., Wood, B.E. The α Centauri line of sight: D/H ratio, physical properties of local interstellar gas, and measurement of heated hydrogen near the heliopause. Astrophys. J. 463, 254–270, 1996.

Mestel, L. Angular momentum loss during pre-main sequence contraction, in: Baliunas, S.L., Hartmann, L. (Eds.), Cool stars, stellar systems, and the Sun, third workshop. Springer, Berlin, pp. 49–59, 1984.

Müller, H.-R., Zank, G.P., Lipatov, A.S. Self-consistent hybrid simulations of the interaction of the heliosphere with the local interstellar medium. J. Geophys. Res. 105, 27419–27438, 2000.

Müller, H.-R., Zank, G.P., Wood, B.E. Modeling the interstellar medium-stellar wind interactions of Lambda Andromedae Epsilon Indi. Astrophys. J. 551, 495–506, 2001.

Sackmann, I.-J., Boothroyd, A.I. Our Sun. V. A bright young Sun consistent with helioseismology and warm temperatures on ancient Earth and Mars. Astrophys. J. 583, 1024–1039, 2003.

Sagan, C., Mullen, G. Earth and Mars: evolution of atmospheres and surface temperatures. Science 177, 52–56, 1972.

Stepień, K. Spin-down of cool stars during their main-sequence life. Astrophys. J. 335, 907–913, 1988.

Vidal-Madjar, A., Lemoine, M., Ferlet, R., et al. Detection of spatial variations in the D/H ratio in the local interstellar medium. Astron. Astrophys. 338, 694–712, 1998.

Wood, B.E., Alexander, W.R., Linsky, J.L. The properties of the local interstellar medium and the interaction of the stellar winds of Epsilon Indi and Lambda Andromedae with the interstellar environment. Astrophys. J. 470, 1157–1171, 1996.

Wood, B.E., Linsky, J.L. The local ISM and its interaction with the winds of nearby late-type stars. Astrophys. J. 492, 788–803, 1998.

Wood, B.E., Linsky, J.L., Müller, H.-R., et al. Observational estimates for the mass-loss rates of a Centauri and Proxima Centauri using Hubble Space Telescope Lyman-α spectra. Astrophys. J. 547, L49–L52, 2001.

Wood, B.E., Linsky, J.L., Müller, H.-R., et al. A search for astrospheric Lyman-α emission around 40 Eri A. Bull. Amer. Astro. Soc. 34, 770, 2002b.

Wood, B.E., Linsky, J.L., Zank, G.P. Heliospheric, astrospheric, and interstellar Lyman-α absorption towards 36 Ophiuchi. Astrophys. J. 537, 304–311, 2000a.

Wood, B.E., Müller, H.-R., Zank, G.P. Hydrogen Lyman-α absorption predictions by Boltzmann models of the heliosphere. Astrophys. J. 542, 493–503, 2000b.

Wood, B.E., Müller, H.-R., Zank, G.P., et al. Measured mass-loss rates of solar-like stars as a function of age and activity. Astrophys. J. 574, 412–425, 2002a.

Zank, G.P., Pauls, H.L., Williams, L.L., et al. Interaction of the solar wind with the local interstellar medium: a multifluid approach. J. Geophys. Res. 101, 21639–21656, 1996.